PHYSICAL REVIEW B **105**, 224107 (2022)

Superconductivity in compressed ternary alkaline boron hydrides

Simin Li,[1,2] Haiyan Wang,[1,*] Weiguo Sun,[2,†] Cheng Lu,[3] and Feng Peng[2,‡]
[1]*School of Materials Science and Engineering, Henan Polytechnic University, Jiaozuo 454000, China*
[2]*College of Physics and Electronic Information & Henan Key Laboratory of Electromagnetic Transformation and Detection, Luoyang Normal University, Luoyang 471022, China*
[3]*School of Mathematics and Physics, China University of Geosciences (Wuhan), Wuhan 430074, China*

(Received 24 January 2022; revised 12 April 2022; accepted 1 June 2022; published 10 June 2022)

Recently, the carbonaceous sulfur hydride was synthesized [E. Snider *et al.*, Nature (London) **586**, 373 (2020)], and the measured superconducting transition temperature (T_c) is about 278 K under 267 GPa, placing it as a promising candidate of the room temperature superconductor. However, the ultrahigh synthesis pressure is indeed a challenge for experimental technique, stimulating us to search other high temperature superconductors under relatively low pressure. Here we perform comprehensively structural searches of ternary alkaline (Am) boron hydrides. Our calculations indicate that the ternary AmB_2H_8 hydrides are energetically stable at about 10 GPa. Interestingly, the metallic Rb/CsB_2H_8 polyhydrides are superior superconductors with high T_c of $\sim$100 K at 25 GPa. The electron-phonon coupling calculations suggest that the Am atoms are promising electron contributors, which effectively improve the T_c and decrease the synthesized pressure in complex hydrides. These findings elucidate the superconductivity mechanism of AmB_2H_8 hydrides and offer crucial insights for design and synthesis of novel superconductors.

DOI: 10.1103/PhysRevB.105.224107

I. INTRODUCTION

The search of novel structure with high superconductivity in polyhydrides has attracted great interest in previous decades, since Ashcroft [1] proposed that the compressed hydrogen-rich compounds are good high-temperature superconductivity materials. A lot of hydrogen-rich compounds containing main group elements are predicted to be potential superconductors with high T_c (such as, 235 K for CaH_6 at 150 GPa [2], 28 K for SiH_4 at 400 GPa [3], 64 K for GeH_4 at 220 GPa [4], 191–204 K for $(H_2S)_2H_2$ at 200 GPa [5], 82 K for LiH_6 at 300 GPa [6], 70 K for KH_6 at 166 GPa [7], 38 K for BeH_2 at 250 GPa [8], and so on [9–11]). Recently, a sulfur hydrides system with high T_c up to 203 K [12] has been obtained by experimental synthesis under 200 GPa, which have been earlier reported by theoretical structure prediction [5,13] within the framework of Bardeen-Cooper-Schrieffer (BCS) theory [14] at high pressures. The superconductive mechanism as well as its possible decompositions of H_2S at high pressure are substantially explored by Duan *et al.* [5]. Subsequently, a series of other group (VA, VIA, and VIIA) hydrides, like H-Se, H-Te, H-Po, H-Br, H-P, H-Sb, etc., are confirmed to be the good superconductors with high T_c in the range of 40–131 K at high pressure, which are pushed by the excited H_3S [12]. To the best of our knowledge, the binary high T_c superconductors are prosperous in compressed polyhydrides containing the main group elements [15], transition metals [16], and rare-earth (RE) metals [17,18]. Especially, our successfully predicated binary high T_c RE hydrides of LaH_{10} [17] at high pressure are directly confirmed by the following experiments [19–24].

A lot of ternary polyhydrides with sizable superconducting transform temperature are reported at high pressure [25–33]. Based on CALYPSO structural prediction method, Sun *et al.* [34] have suggested that the estimated T_c of $LiMg_2H_{16}$ hydride is remarkably high to about 473 K at 250 GPa [34]. Ternary carbonaceous sulfur hydride has attracted extensive attention due to the high T_c up to room temperature (about 287 K) [35]. Meanwhile, there are some discrepancies between theoretical and experiment results, which include the singularly sharp superconducting transition under an external magnetic field [36–38] and uncertain crystals structures for C-S-H systems [39]. Other ternary hydrides are also discovered, for example $YCaH_{12}$ ($T_c \sim 230$ K at 180 GPa) [27–30] $(La,Y)H_{10}$ ($T_c \sim 253$ K at 183 GPa) [40], and $LiPH_6$ ($T_c \sim 167$ K at 200 GPa) [29]. However, these synthesized and stable pressures are ultrahigh, and it is still a challenge to achieve and hold such enormous pressure in experiment. Very recently, Zhang *et al.* have reported a class of the AXH_8-type hydrogen-based alloy backbone (e.g., $LaBeH_8$ with sizable $T_c \sim 185$ K), which could further reduce the stable pressure of hydrogen-based superconductors at moderate pressure (20 GPa) [41]. Thus, the search of the potential ternary hydrides with high T_c at moderate or ambient pressure is the hot topic in high pressure physics.

The electronic properties of hydrogen-rich superconductors reveal two primary conclusions: (I) the metallic H-H σ covalent bonds formed by charge transfer from metal atoms always induce the high T_c but at ultrahigh pressure due to the large contributions to the density of states (DOS) around the Fermi level and (II) the metallic other H σ covalent bonds formed by introducing the light mass nonmetal

---

[*] wanghy@hpu.edu.cn
[†] xwswguo@163.com
[‡] fpeng@calypso.cn

elements (e.g., sulfur) usually bring the moderate T_c at relatively low pressure. Through a full exploration of the light elements, for instance, boron, carbon, nitrogen, and phosphorus based hydrides, boron is amazedly found to be easily formed by the metallic σ bonds with H atom because of its electron deficiency.

In this work we systematically perform structural searches for alkaline boron hydrides AmB_2H_8 (Am = Li, Na, K, Rb, and Cs) under high pressure from 10 to 100 GPa. A series of energetically stable and metallic hydrides with stoichiometries of KB_2H_8, RbB_2H_8 and CsB_2H_8 are uncovered. Moreover, the predicted KB_2H_8, RbB_2H_8 and CsB_2H_8 hydrides are identified to be formed by the BH_4 tetrahedrons located in the framework of Am lattices, and found to be excellent high-temperature superconductors at relatively lower pressure.

II. COMPUTATIONAL DETAILS

We have performed the detailed structural predictions for KB_2H_8 crystal under the high pressure 0, 10, 25, 50, and 100 GPa with 1–4 formula units (f.u.) per cell by CALYPSO [42,43] method associated with first-principal calculations. During our structure searches, most searches converge in 50 generations and the total number of predicted structures is about 2500 structures generated. We have also constructed the other AmB_2H_8 (Am = Li, Na, Rb, and Cs) crystal hydrides referred to KB_2H_8 structure information. The enthalpies and electronic properties of candidate structures of AmB_2H_8 hydrides are realized by Vienna *ab initio* simulation package (VASP) code [44] using the projected augmented wave (PAW) potentials [45] with Perdew-Burke-Ernzerhof (PBE) [46] exchange-correlation functions. The $1s^1$, $2s^2 2p^1$, and $ns^2 np^6 (n+1)s^1$ valence configurations are treated as valence electrons for H, B, and Am atoms, respectively. The tested energy cutoff of 700 eV and dense Monkhorst-Pack [47] k meshes with grid spacing of $2\pi \times 0.02$ in the Brillouin zone are chosen to ensure all the structures are converged with the enthalpy less than 1 meV/atom. The electron-phonon coupling parameters and phonon dispersion curves are calculated by the QUANTUM-ESPRESSO package [48] with density functional perturbation theory (DFPT). The ultrasoft pseudopotentials of H, B, and Am atoms are considered with a kinetic energy cutoff of 100 Ry. The $6 \times 6 \times 6$ q meshes and dense $24 \times 24 \times 24$ k point are adopted in the EPC calculations. The T_c was estimated by the Allen-Dynes modified McMillan equation [49],

$$T_c = \frac{\omega_{\log}}{1.2} \exp\left[\frac{-1.04(1+\lambda)}{\lambda - \mu^*(1+0.62\lambda)}\right], \tag{1}$$

which is also considered strong-coupling and shape correction multipliers (f_1 and f_2) with calculation

$$f_1 = \left[1 + \left(\frac{\lambda}{2.46(1+3.8\mu^*)}\right)^{3/2}\right]^{1/3}, \tag{2}$$

$$f_2 = 1 + \frac{\left(\frac{\bar{\omega}}{\omega_{\log}} - 1\right)\lambda^2}{\lambda^2 + \left[1.82(1+6.3\mu^*)\frac{\bar{\omega}}{\omega_{\log}}\right]^2}, \tag{3}$$

$$T_c = f_1 f_2 \frac{\omega_{\log}}{1.2} \exp\left(\frac{-1.04(1+\lambda)}{\lambda - \mu^*(1+0.62\lambda)}\right), \tag{4}$$

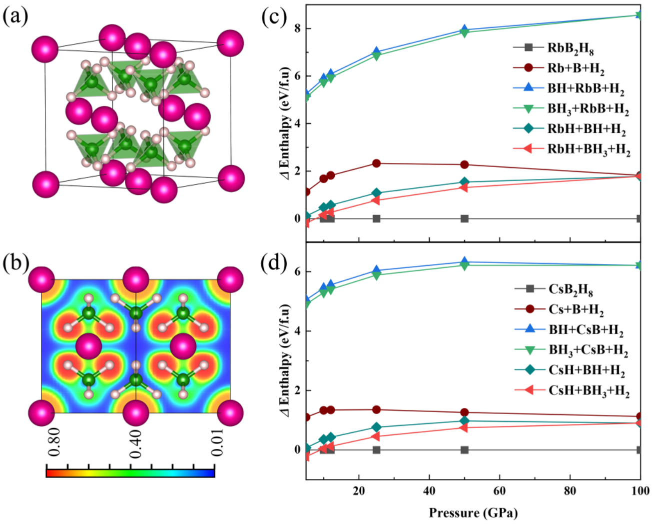

FIG. 1. (a) The crystal structures of AmB_2H_8 hydrides. The magenta, green, and pink balls represent the alkaline metal (K, Rb,and Cs), boron, and hydrogen atoms, respectively. (b) The ELFs of RbB_2H_8 in (110) plane at 25 GPa. (c) and (d) The calculated formation enthalpies (ΔH) of Rb/CsB_2H_8 hydrides as a function of pressure at 5, 10, 12, 25, 50, and 100 GPa. (c) RbB_2H_8 and (d) CsB_2H_8.

where the logarithmic average frequency $\omega_{\log}$ and mean square frequency $\bar{\omega}_{\log}$ are defined as

$$\omega_{\log} = \exp\left[\frac{\lambda}{2}\int \ln(\omega)\frac{\alpha^2F(\omega)}{\omega}d(\omega)\right], \tag{5}$$

$$\bar{\omega} = \sqrt{\frac{2}{\lambda}\int \alpha^2F(\omega)\omega d(\omega)}. \tag{6}$$

The crystal structures and electron localization functions are visualized by VESTA software [50].

III. RESULTS AND DISCUSSION

We explore the stable structures of various AmB_2H_8 hydrides at high pressure. The enthalpy of per atom for different KB_2H_8 phase with respect to $Fm\bar{3}m$ structure has been displayed in Fig. S1 in the Supplemental Material (SM) [51], which indicated that the cubic $Fm\bar{3}m$ KB_2H_8 are mostly stable structures at high pressure. The detailed structure information including $I4_1/a$, $I4_1/amd$, $Pmm2$, and $P\bar{6}$ also have been collected in Table S1 [51]. The crystal structures of cubic AmB_2H_8 hydrides are depicted in Figs. 1(a) and S2(b). Eight BH_4 tetrahedrons are located in the frameworks of the fcc Am lattices at low pressure. The B-H bond length of different AmB_2H_8 hydrides are about 1.229–1.239 Å at 10 GPa, and 1.165–1.200 Å at 100 GPa, respectively. The chemical bonding characteristics of BH_4 tetrahedrons are checked by the electron localization functions (ELF), as shown in Fig. 1(b). The electrons are clearly localized between B-H bonds and close to the H atoms in the (110) plane of RbB_2H_8 hydrides. Similar behaviors are also found in other AmB_2H_8 hydrides. The projected crystal orbital Hamiltonian population (pCOHP) of the KB_2H_8, RbB_2H_8 and CsB_2H_8 compounds at 12 and 25 GPa have been displayed in Fig. S3 [51], which signify the strong B-H bonding states in AmB_2H_8 systems. The analyses of Bader charges reveal that the H atoms accept the $0.51e$ electron form Am and boron atoms, which indicate the strong B-H bond in BH_4 tetrahedrons. The detailed charge transfer results are shown in Table S2 [51]. Meanwhile, the energetically stable Rb/CsB_2H_8 hydrides are also evaluated through their formation enthalpies relative to the possible products of dissociation into corresponding atoms and binary compounds under 5, 10, 12, 25, 50, and 100 GPa. In our calculations we used $Fm\bar{3}m$ for Rb/CsH [52], $C2/c$ for BH [53], $P2_1/c$ for BH_3 [53], and $P6_3/m$ for H_2 [54] at 0–100 GPa. The calculated results are depicted in Figs. 1(c) and 1(d). The results of decomposition products exhibit the positive values of formation enthalpies relative to AmB_2H_8 hydrides, suggesting the thermodynamically stable Rb/CsB_2H_8 at pressures from 10 to 100 GPa. The detailed phonon dispersion curves show that the alkaline Li/NaB_2H_8 hydrides are dynamically instability at 10–100 GPa (see Fig. S4 [51]). By contrast, AmB_2H_8 (Am = K, Rb, and Cs) are stable above 10 GPa, as shown in Figs. S5 and S6 [51]. Gao *et al.* have reported the detailed electron properties KB_2H_8 hydride at 12 GPa [31]. Here we mainly focus on the predicted structures of post alkaline Rb/CsB_2H_8 hydrides.

In order to reveal the fascinating properties of Rb/CsB_2H_8, we carry out the calculations of electronic band structures combined with their projected densities of states for the stable structures at 15, 25, and 50 GPa, as shown in Figs. 2 and S7, respectively. It can be clearly seen that the ground state structures of Rb/CsB_2H_8 are metallic with several bands crossing the Fermi level (N_F) in both electronic band curves. The large density states around N_F are primarily contributed from the apparent hybridization of B-*p* and H-*s* orbitals at Fermi level. Obviously there are huge energy gaps within the energy range from Fermi level to 6 eV for both RbB_2H_8 and CsB_2H_8 at different pressures. Furthermore, the pierced bands near the N_F with the features of flat bands and steep bands [see Figs. 2(a) and 2(b)] verify that Rb/CsB_2H_8 hydrides are potential superconductors [55].

To elucidate the superconductivity and the underlying mechanism, we calculate the phonon dispersion curves, phonon density of states (PHDOS) projected on Rb/Cs and H atoms, Eliashberg spectral function $\alpha^2F(\omega)$ and electron-phonon coupling (EPC) integrated $\lambda(\omega)$ of Rb/CsB_2H_8 hydrides at 25 GPa. The calculated results are displayed in Figs. 3(a) and 3(c). Both RbB_2H_8 and CsB_2H_8 hydrides are represented by similar characteristics. From Figs. 3(a) and 3(c) a gap of about 1000 cm^{-1} is found at around 1000 cm^{-1}, which separates the phonon bands into two parts for both RbB_2H_8 and CsB_2H_8 hydrides. The low frequency parts including the low frequency optical branches and acoustic modes derived from the vibrations of heavy mass of Rb/Cs and B atoms are below 500 cm^{-1}, while the high frequency optical branches are mainly associated with H atoms [see Fig. 3(a)]. Meanwhile, the Fermi surfaces of Rb/CsB_2H_8 at 25 GPa, as shown in Figs. 3(b) and 3(d), reveal the electron pockets around Gamma point. As for RbB_2H_8 hydride, the low frequency modes below 500 cm^{-1} contribute about 16.5% to the EPC parameter λ, whereas the remaining 83.5% of the total value of λ are sourced by the high frequency modes, which are produced by the BH_4 tetrahedrons [see Fig. 3(a)]. Meanwhile, the Eliashberg spectral functions $\lambda(\omega)$ revealing the high frequency of H vibrations in CsB_2H_8 hydride provide about 66.1% contributions to λ when the frequencies are higher than 500 cm^{-1}. Of course Cs atoms also contribute 22.3% to the total EPC parameter λ of 1.836. These calculations reveal that the large fractions of the superconductivity are induced by the vibrations of B/H atoms, while the Rb/Cs atoms contribute relatively little fractions.

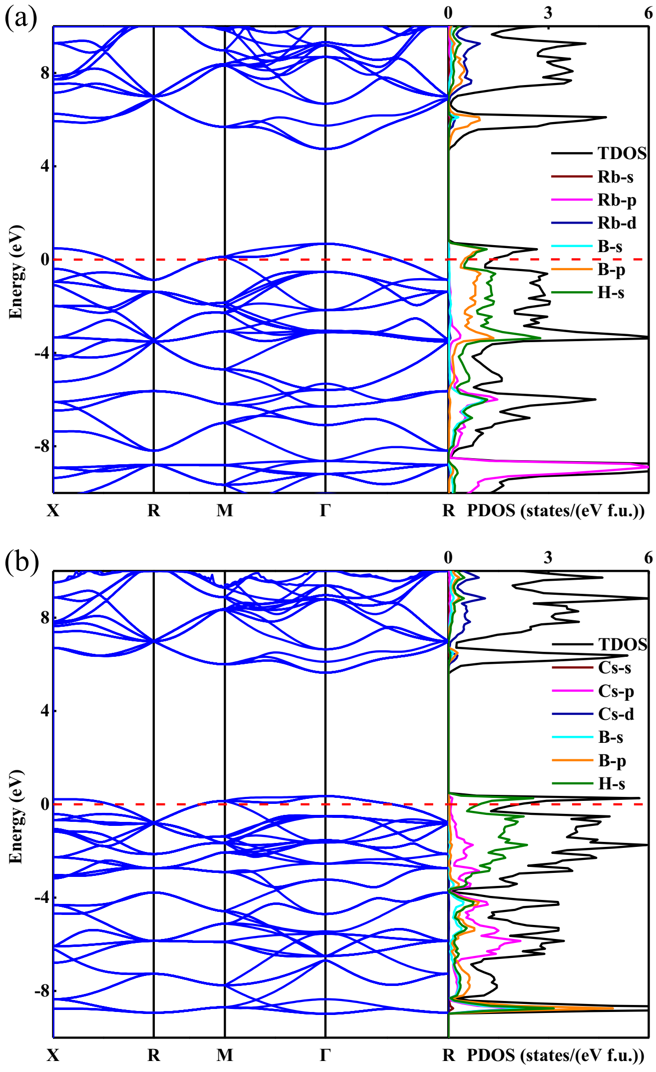

FIG. 2. The calculated electronic band structures and projected densities of states of (a) RbB_2H_8 and (b) CsB_2H_8 at 25 GPa.

In exploring the superconducting properties on AmB_2H_8 hydrides, we calculate the critical temperature of T_c by solving the Eliashberg equations [56] based on the spectral functions of $\alpha^2F(\omega)$ and a typically selected Coulomb pseudopotential of μ^* [57]. The superconducting properties of AmB_2H_8 hydrides at different pressure are summarized in Table I, together with the estimated T_c values from the modified McMillan and Allen-Dynes equation when the EPC parameters λ are larger than 1.5 (see Fig. 4). At 25 GPa, the predicted T_c of KB_2H_8 reaches a medium 100.6 K with a slightly smaller λ of 1.613. With a decrease of pressure, the T_c shows an abnormal increase of the superconducting transition temperature, which

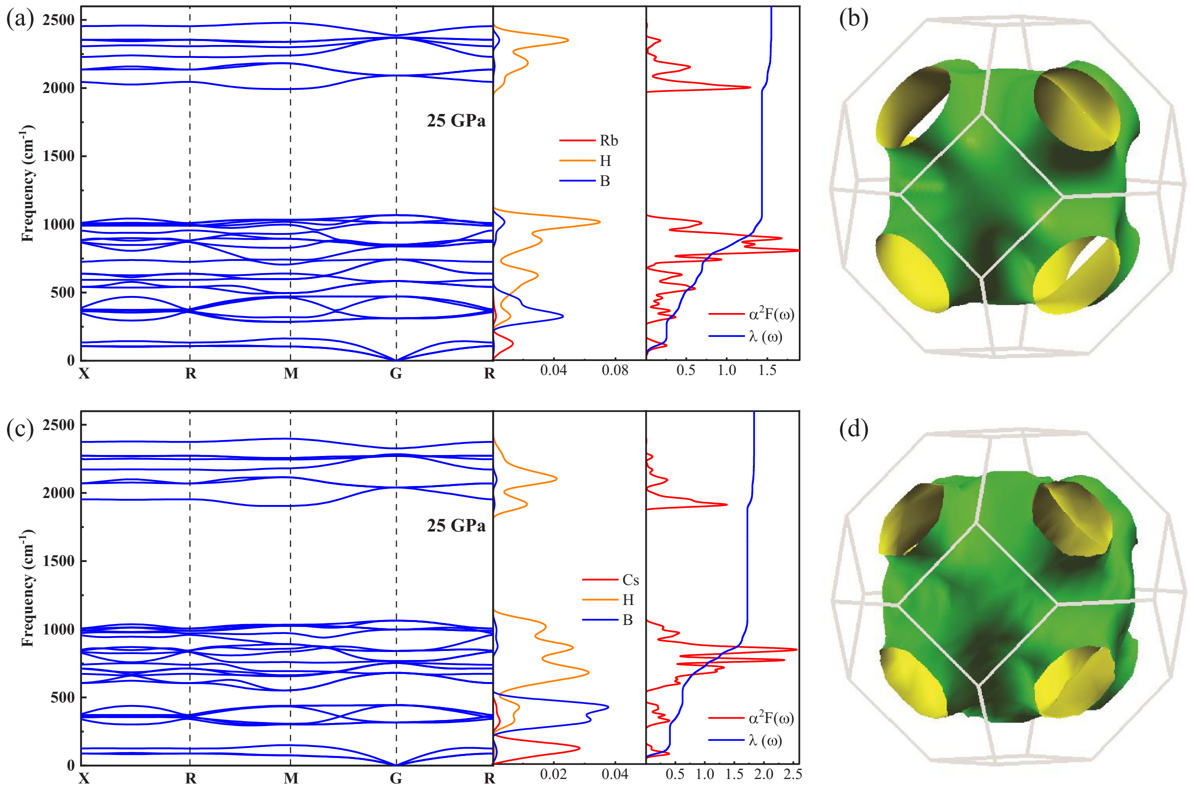

FIG. 3. The calculated phonon dispersion curves, phonon density of states (PHDOS), and Eliashberg spectral function $\alpha^2F(\omega)$ together with the electron-phonon coupling (EPC) integral $\lambda(\omega)$ of Rb/CsB_2H_8 hydrides. (a) RbB_2H_8 at 25 GPb, (c) CsB_2bH_8 at 25 GPa. The calculated Fermi surfaces of Rb/CsB_2H_8 hydrides. (b) RbB_2H_8 at 25 GPa, (d) CsB_2H_8 at 25 GPa.

is about 134 K at 12 GPa [31]. As for RbB_2H_8, the value of λ decreases to 1.051 at 50 GPa, leading to the decrease of T_c to 75.42 K with $\mu^* = 0.1$. The highest T_c of RbB_2H_8 hydride is found to be 104.8 K at 25 GPa. The calculated T_c of CsB_2H_8 hydride in the pressure range of 15 to 50 GPa are about 52.7 to 68.7 K with λ varied from 2.138 to 1.088. However, a highest critical temperature of 106.0 K for CsB_2H_8 at 25 GPa is obtained by solving the Allen-Dynes modified McMillan equation and the corresponding EPC parameter λ is 1.836. The moderate increase of T_c among AmB_2H_8 (Am = K, Rb, and Cs) hydrides at 25 GPa might be due to the gradual decrease of the electronegativity properties of alkaline metal elements. Our calculations reveal that the high superconducting temperature T_c up to 106.0 K for CsB_2H_8 can be achieved at extremely low pressure of 25 GPa, and the Cs atoms are electron contributors, essentially improving T_c and decreasing the stable pressure of CsB_2H_8 hydride. Further experimental works are needed to better understand superconductivity of these ternary alkaline boron hydrides.

IV. CONCLUSIONS

In summary, we have predicted the ground state structures of AmB_2H_8 hydrides under high pressure based on

TABLE I. The superconducting properties of AmB_2H_8 (Am = K, Rb, and Cs) at different pressures. The values of T_c are estimated by the McMillan equation and the Allen-Dynes modified McMillan equation.

				T_c (K)		$f_1f_2T_c$ (K)
Hydrides	Pressure (GPa)	λ	$\omega_{\log}$ (K)	$\mu^* = 0.10$	$\mu^* = 0.13$	$\mu^* = 0.10$
KB_2H_8	25	1.613	705.02	85.86	78.84	100.60
RbB_2H_8	15	2.210	509.56	78.19	73.40	100.91
	25	1.550	770.02	90.52	82.82	104.79
	50	1.051	1006.00	75.42	65.39	
	100	0.865	1146.28	62.57	51.80	
CsB_2H_8	15	2.138	350.78	52.73	49.41	67.29
	25	1.836	647.02	87.52	81.22	106.03
	50	1.088	871.38	68.66	59.92	
	100	0.922	1017.65	62.14	52.33	

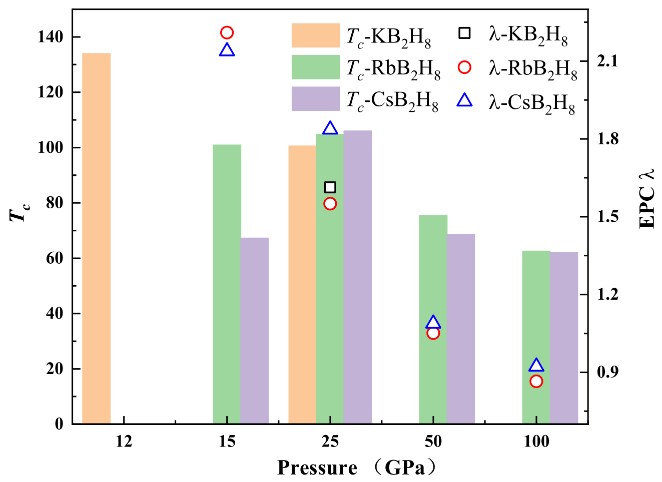

FIG. 4. The calculated electron-phonon coupling (EPC) parameters λ (dotted line relative to right axis) and superconducting temperature T_c (column relative to left axis) as functions of pressure for KB_2H_8, RbB_2H_8, and CsB_2H_8 at 12, 15, 25 50, and 100 GPa. The T_c of KB_2H_8 at 12 GPa are 134 K [31].

CALYPSO method and first-principle calculations. The calculated enthalpies and phonon dispersion curves verify that the KB_2H_8, RbB_2H_8, and CsB_2H_8 hydrides are thermodynamically stable above 12 GPa. Most importantly, the metallic Rb/CsB_2H_8 hydrides are superior superconductors with a high T_c of ∼100 K at 25 GPa. The electron-phonon coupling calculations indicate that the H atoms or BH_4 tetrahedrons in Rb/CsB_2H_8 contribute the large fractions to the total values of integrated λ, and the Am atoms are outstanding electron contributors, which enormously decrease the synthesized pressure in polyhydrides. These results offer important avenues for experimental synthesis of novel hydrogen-based superconductors.

ACKNOWLEDGMENTS

This work is supported by the National Natural Science Foundation of China under Grants No. 12111530103, No. 11774140, No. 12174352, and No. 12174170, the Program for Science and Technology Innovation Research Team in University of Henan Province under Grant No. 17HASTIT015, the Higher Levels of Young Teachers Funding Scheme of Henan Province Grant No. 2019GGJS057, the Key Scientific Research Projects of Colleges and Universities in Henan Province Grants No. 20A430017 and No. 22A140025, and the Postdoctoral Science Foundation of Henan Province.

---

[1] N. W. Ashcroft, Phys. Rev. Lett. **21**, 1748 (1968).
[2] H. Wang, J. S. Tse, K. Tanaka, T. Iitaka, and Y. Ma, Proc. Natl. Acad. Sci. USA **109**, 6463 (2012).
[3] K. Abe, Phys. Rev. B **103**, 134118 (2021).
[4] G. Gao, A. R. Oganov, A. Bergara, M. Martinez-Canales, T. Cui, T. Iitaka, Y. Ma, and G. Zou, Phys. Rev. Lett. **101**, 107002 (2008).
[5] D. Duan, Y. Liu, F. Tian, D. Li, X. Huang, Z. Zhao, H. Yu, B. Liu, W. Tian, and T. Cui, Sci. Rep. **4**, 6968 (2015).
[6] Y. Xie, Q. Li, A. R. Oganov, and H. Wang, Acta Crystallogr. C Struct. Chem. **70**, 104 (2014).
[7] D. Zhou, X. Jin, X. Meng, G. Bao, Y. Ma, B. Liu, and T. Cui, Phys. Rev. B **86**, 014118 (2012).
[8] C. Zhang, X. J. Chen, R. Q. Zhang, and H. Q. Lin, J. Phys. Chem. C **114**, 14614 (2010).
[9] J. S. Tse, Y. Yao, and K. Tanaka, Phys. Rev. Lett. **98**, 117004 (2007).
[10] G. Gao, A. R. Oganov, P. Li, Z. Li, H. Wang, T. Cui, Y. Ma, A. Bergara, A. O. Lyakhov, T. Iitaka, and G. Zou, Proc. Natl. Acad. Sci. USA **107**, 1317 (2010).
[11] I. Goncharenko, M. I. Eremets, M. Hanfland, J. S. Tse, M. Amboage, Y. Yao, and I. A. Trojan, Phys. Rev. Lett. **100**, 045504 (2008).
[12] A. P. Drozdov, M. I. Eremets, I. A. Troyan, V. Ksenofontov, and S. I. Shylin, Nature (London) **525**, 73 (2015).
[13] Y. Li, J. Hao, H. Liu, Y. Li, and Y. Ma, J. Chem. Phys. **140**, 174712 (2014).
[14] J. Bardeen, L. N. Cooper, and J. R. Schrieffer, Phys. Rev. **108**, 1175 (1957).
[15] E. Zurek and T. G. Bi, J. Chem. Phys. **150**, 050901 (2019).
[16] D. F. Duan, Y. X. Liu, Y. B. Ma, Z. Shao, B. B. Liu, and T. Cui, Nat. Sci. Rev. **4**, 121 (2017).
[17] F. Peng, Y. Sun, C. J. Pickard, R. J. Needs, Q. Wu, and Y. Ma, Phys. Rev. Lett. **119**, 107001 (2017).
[18] W. Sun, X. Kuang, H. D. J. Keen, C. Lu, and A. Hermann, Phys. Rev. B **102**, 144524 (2020).
[19] A. Drozdov, P. Kong, V. Minkov, S. Besedin, M. Kuzovnikov, S. Mozaffari, L. Balicas, F. Balakirev, D. Graf, and V. Prakapenka, Nature (London) **569**, 528 (2019).
[20] M. Somayazulu, M. Ahart, A. K. Mishra, Z. M. Geballe, M. Baldini, Y. Meng, V. V. Struzhkin, and R. J. Hemley, Phys. Rev. Lett. **122**, 027001 (2019).
[21] W. Chen, D. V. Semenok, X. Huang, H. Shu, X. Li, D. Duan, T. Cui, and A. R. Oganov, Phys. Rev. Lett. **127**, 117001 (2021).
[22] D. Zhou, D. V. Semenok, H. Xie, X. Huang, D. Duan, A. Aperis, P. M. Oppeneer, M. Galasso, A. I. Kartsev, A. G. Kvashnin, A. R. Oganov, and T. Cui, J. Am. Chem. Soc. **142**, 2803 (2020).
[23] P. Kong, V. S. Minkov, M. A. Kuzovnikov, A. P. Drozdov, S. P. Besedin, S. Mozaffari, L. Balicas, F. F. Balakirev, V. B. Prakapenka, S. Chariton, D. A. Knyazev, E. Greenberg, and M. I. Eremets, Nat. Commun. **12**, 5075 (2021).
[24] L. Ma, M. Zhou, Y. Wang, S. Kawaguchi, Y. Ohishi, F. Peng, H. Liu, G. Liu, H. Wang, and Y. Ma, Phys. Rev. Research **3**, 043107 (2021).
[25] J. Zheng, W. Sun, X. Dou, A.-J. Mao, and C. Lu, J. Phys. Chem. C **125**, 3150 (2021).
[26] P. Zhang, Y. Sun, X. Li, J. Lv, and H. Liu, Phys. Rev. B **102**, 184103 (2020).
[27] H. Xie, D. Duan, Z. Shao, H. Song, Y. Wang, X. Xiao, D. Li, F. Tian, B. Liu, and T. Cui, J. Phys.: Condens. Matter **31**, 245404 (2019).
[28] Y. Sun, Y. Tian, B. Jiang, X. Li, H. Li, T. Iitaka, X. Zhong, and Y. Xie, Phys. Rev. B **101**, 174102 (2020).

[29] Z. Shao, D. Duan, Y. Ma, H. Yu, H. Song, H. Xie, D. Li, F. Tian, B. Liu, and T. Cui, Npj Comput. Mater. **5**, 104 (2019).

[30] X. Liang, A. Bergara, L. Wang, B. Wen, Z. Zhao, X.-F. Zhou, J. He, G. Gao, and Y. Tian, Phys. Rev. B **99**, 100505(R) (2019).

[31] M. Gao, X. W. Yan, Z.-Y. Lu, and T. Xiang, Phys. Rev. B **104**, L100504 (2021).

[32] W. Cui, T. Bi, J. Shi, Y. Li, H. Liu, E. Zurek, and R. J. Hemley, Phys. Rev. B **101**, 134504 (2020).

[33] X. Liang, A. Bergara, X. Wei, X. Song, L. Wang, R. Sun, H. Liu, R. J. Hemley, L. Wang, G. Gao, and Y. Tian, Phys. Rev. B **104**, 134501 (2021).

[34] Y. Sun, J. Lv, Y. Xie, H. Liu, and Y. Ma, Phys. Rev. Lett. **123**, 097001 (2019).

[35] E. Snider, N. Dasenbrock-Gammon, R. McBride, M. Debessai, H. Vindana, K. Vencatasamy, K. V. Lawler, A. Salamat, and R. P. Dias, Nature (London) **586**, 373 (2020).

[36] J. E. Hirsch and F. Marsiglio, Nature (London) **596**, E9 (2021).

[37] J. E. Hirsch and F. Marsiglio, Phys. Rev. B **103**, 134505 (2021).

[38] J. Hirsch, arXiv:2109.08517.

[39] M. Gubler, J. A. Flores-Livas, A. Kozhevnikov, and S. Goedecker, Phys. Rev. Materials **6**, 014801 (2022).

[40] D. V. Semenok, I. A. Troyan, A. G. Ivanova, A. G. Kvashnin, I. A. Kruglov, M. Hanfland, A. V. Sadakov, O. A. Sobolevskiy, K. S. Pervakov, I. S. Lyubutin, K. V. Glazyrin, N. Giordano, D. N. Karimov, A. L. Vasiliev, R. Akashi, V. M. Pudalov, and A. R. Oganov, Mater. Today **48**, 18 (2021).

[41] Z. Zhang, T. Cui, M. J. Hutcheon, A. M. Shipley, H. Song, M. Du, V. Z. Kresin, D. Duan, C. J. Pickard, and Y. Yao, Phys. Rev. Lett. **128**, 047001 (2022).

[42] Y. C. Wang, J. Lv, L. Zhu, and Y. Ma, Comput. Phys. Commun. **183**, 2063 (2012).

[43] Y. C. Wang, J. Lv, L. Zhu, and Y. M. Ma, Phys. Rev. B **82**, 094116 (2010).

[44] G. Kresse and J. Furthmüller, Phys. Rev. B **54**, 11169 (1996).

[45] G. Kresse and D. Joubert, Phys. Rev. B **59**, 1758 (1999).

[46] J. P. Perdew, K. Burke, and M. Ernzerhof, Phys. Rev. Lett. **77**, 3865 (1996).

[47] H. J. Monkhorst and J. D. Pack, Phys. Rev. B **13**, 5188 (1976).

[48] P. Giannozzi, S. Baroni, N. Bonini, M. Calandra, R. Car, C. Cavazzoni, D. Ceresoli, G. L. Chiarotti, M. Cococcioni, I. Dabo, A. Dal Corso, S. de Gironcoli, S. Fabris, G. Fratesi, R. Gebauer, U. Gerstmann, C. Gougoussis, A. Kokalj, M. Lazzeri, L. Martin-Samos, N. Marzari *et al.*, J. Phys.: Condens. Matter **21**, 395502 (2009).

[49] P. B. Allen and R. C. Dynes, Phys. Rev. B **12**, 905 (1975).

[50] K. Momma and F. Izumi, J. Appl. Crystallogr. **44**, 1272 (2011).

[51] See Supplemental Material at http://link.aps.org/supplemental/10.1103/PhysRevB.105.224107 for calculated phonon dispersions, band structure, densities of states, Bader charges, and structural parameters for predicted AmB_2H_8 hydrides.

[52] J. Hooper, P. Baettig, and E. Zurek, J. Appl. Phys. **111**, 112611 (2012).

[53] C. H. Hu, A. R. Oganov, Q. Zhu, G. R. Qian, G. Frapper, A. O. Lyakhov, and H. Y. Zhou, Phys. Rev. Lett. **110**, 165504 (2013).

[54] C. J. Pickard and R. J. Needs, Nat. Phys. **3**, 473 (2007).

[55] A. Simon, Angew. Chem. Int. Ed. Engl. **36**, 1788 (1997).

[56] G. Eliashberg, Sov. Phys. JETP **11**, 696 (1960).

[57] Y. Yao, J. S. Tse, K. Tanaka, F. Marsiglio, and Y. Ma, Phys. Rev. B **79**, 054524 (2009).